A negative derivative feedback design algorithm

F Cola, F Resta and F Ripamonti

Politecnico di Milano, Mechanical Engineering Department, Via La Masa 1, 20156 Milano, Italy

E-mail: francesco.ripamonti@polimi.it

Received 16 April 2014
Accepted for publication 7 May 2014
Published 18 June 2014

1. Introduction

Vibration reduction in mechanical and civil structures has always represented an important target, since stresses introduced by dynamic amplifications can induce failures and reduce performance. The need to design light structures with consequently low damping in many fields such as aerospace, transport and, in general, all those applications in which it is convenient to save materials or energy, has made the problem more acute. For these reasons, both passive and active solutions have been proposed for reducing vibrations, particularly in the case of resonance forcing conditions. Among the passive solutions is the dynamic absorber, a one degree of freedom (d.o.f.) device consisting of a mass connected by elastic-viscous elements to the main system and tuned on a natural frequency, as well as its extension to multi-d.o.f. Recently, however, the increasing availability of sensors and actuators has given considerable impetus to active vibration control. Among the control logics developed for reducing dynamic amplifications in resonance conditions, independent modal space control (IMSC) [1] makes it possible, under certain assumptions, to act on different modes independently increasing damping. The most important limit of this strategy is the spillover effect, due to the presence of unmodelled modes, which can lead to degradation of performance or even instability [2]. To reduce spillover, a family of control logics, known as 'resonant control', has been developed. The characteristic of these strategies is the evaluation of the control action through a dynamic system (usually a first or second order compensator) so that the force applied to the system is opposite in phase to the modal velocity corresponding to the controlled mode resonance frequency. One of the first resonant controls was positive position feedback (PPF), developed by Goh and Caughey [3]. To avoid high frequency spillover, the generalized displacement is fed back through a second order low-pass filter so that in the neighbourhood of the cut-off frequency the control force has a damping effect. However, at low frequencies this control strategy causes a reduction of stiffness affecting quasi-static performances. Later the strain-rate feedback (SRF) control logic was presented by Agrawal *et al* [4]. In this case, the control action is obtained by filtering the generalized velocity with a second order low-pass filter the generalized velocity. This way, a damping effect is obtained before the cut-off frequency, while above this frequency the control force results in a negative damping. More recently, a resonant control, called active modal tuned mass damper (AMTMD) [5], was designed to reproduce the behaviour of a passive mechanical tuned mass

damper. In this case, the transfer function between modal velocity and control force is a high-pass filter reducing spillover at low frequencies. Finally, a control strategy known as negative derivative feedback (NDF) [6] proved more robust against spillover since it acts as a band-pass filter. As mentioned above, all these control strategies make use of compensators whose design involves the setting of a large number of parameters, very often without a precise physical meaning. Except in the case of AMTMD, where control design could rely on the well-known theory of passive mechanical tuned mass dampers [7], there are few guidelines for the definition of these coefficients. For this reason, in this paper a design strategy for a single and multi-d.o.f. NDF controller based on an output feedback control formulation is proposed, by analogy with what has been done for PPF by Inman and Friswell [8]. In section 2, modal space theory and NDF control strategy are described. In sections 3 and 4 the design methodology is described for single and multi-d.o.f. systems. For both cases a numerical test has been developed and is described in section 5.

2. The NDF

Consider a generic mechanical system described by n second order differential equations

$$M\ddot{\mathbf{x}} + R\dot{\mathbf{x}} + K\mathbf{x} = \Lambda^T \mathbf{f}_c + \mathbf{f}_d \tag{1}$$

where

- $\mathbf{x}$ is the $n \times 1$ vector containing the physical coordinates
- M, R, K are respectively the mass, damping and stiffness $n \times n$ matrices
- Λ^T is the Jacobian matrix describing the relationship between displacement of points where control forces are applied and the vector $\mathbf{x}$
- $\mathbf{f}_c$ and $\mathbf{f}_d$ are respectively the control and disturbance forces

To obtain a simpler model with a reduced number of d.o.f., the modal approach can be used, describing the system in the range of frequencies of interest with a set of m principal coordinates $\mathbf{q}$. The modal variables are related to the physical ones by

$$\mathbf{x} = \Phi\mathbf{q} \tag{2}$$

where Φ is the $n \times m$ modal matrix containing the eigenvectors of $M^{-1}K$ associated with the considered modes. Normalizing the eigenvectors to have a unitary mass matrix, a set of m decoupled equations, is obtained (under proper assumptions about the damping matrix)

$$\ddot{q}_i + 2\xi_i\omega_i\dot{q}_i + \omega_i^2 q_i = u_{c_i} + u_{d_i} \tag{3}$$

where i is the modal index while u_{c_i} and u_{d_i} are respectively the control and disturbance force components acting on the ith mode. The relationship between the modal ($\mathbf{u}_c$) and physical ($\mathbf{f}_c$) control forces is expressed as

$$\mathbf{f}_c = \left(\Phi^T\Lambda^T\right)^{-1}\mathbf{u}_c \tag{4}$$

Now it is possible to consider the NDF control logic where the modal force is set equal to the first derivative of an auxiliary variable η_i multiplied by a negative gain

$$u_{c_i} = -g_i\dot{\eta}_i \tag{5}$$

The dynamics of the auxiliary system are described by

$$\ddot{\eta}_i + 2\xi_{f_i}\omega_{f_i}\dot{\eta}_i + \omega_{f_i}^2\eta_i = k_{d_i}\left(\dot{q}_i - \dot{\eta}_i\right) \tag{6}$$

From equations (5) and (6) the transfer function between the modal force and the modal velocity can be derived

$$\frac{u_{c_i}(s)}{\dot{q}_i(s)} = -\frac{k_{d_i}g_i s}{s^2 + \left(2\xi_{f_i}\omega_{f_i} + k_{d_i}\right)s + \omega_{f_i}^2} \tag{7}$$

The expression is that of a band-pass filter. It is possible to demonstrate that this result is responsible for the reduction of spillover effects both at lower and higher frequencies [6].

3. NDF design methodology

Looking at (7), the NDF compensator design involves the setting of the coefficients g_i, k_{d_i}, ξ_{f_i}, ω_i for each controlled mode. Except for ω_{f_i}, which can be tuned on the natural frequency of the controlled mode, there are no developed strategies for the choice of all the other parameters, which also have a weak physical meaning. For this reason, the idea is to formulate the problem as an output feedback control problem [8] so that the control design can be done using an optimal approach.

3.1. Single d.o.f. systems

Consider first the dynamics of a single d.o.f. linear system (neglecting the external disturbance) and the corresponding NDF compensator (whose parameters are identified by the index f)

$$\begin{cases} \ddot{q} + 2\xi\omega\dot{q} + \omega^2 q = u_c = -g\dot{\eta} \\ \ddot{\eta} + 2\xi_f\omega_f\dot{\eta} + \omega_f^2\eta = k_d\left(\dot{q} - \dot{\eta}\right) \end{cases} \tag{8}$$

and define a new set of variables

$$\mathbf{z} = \begin{Bmatrix} q \\ \dot{q} \\ g\eta \\ g\dot{\eta} \end{Bmatrix} \tag{9}$$

It is possible to express (8) in state space form

$$\begin{cases} \dot{\mathbf{z}} &= A\mathbf{z} + B\mathbf{v} \\ \mathbf{y} &= C\mathbf{z} \end{cases} \tag{10}$$

where

$$A = \begin{bmatrix} 0 & 1 & 0 & 0 \\ -\omega^2 & -2\xi\omega & 0 & -1 \\ 0 & 0 & 0 & 1 \\ 0 & 0 & 0 & 0 \end{bmatrix} B = \begin{bmatrix} 0 \\ 0 \\ 0 \\ 1 \end{bmatrix}$$

$$C = \begin{bmatrix} 0 & 1 & 0 & 0 \\ 0 & 0 & 1 & 0 \\ 0 & 0 & 0 & 1 \end{bmatrix} \tag{11}$$

and

$$\mathbf{v} = G\mathbf{y} = \begin{bmatrix} k_d\, g & -\omega_f^2 & -2\xi_f\omega_f - k_d \end{bmatrix}\mathbf{y} \tag{12}$$

In this way, all the unknown design parameters appear exclusively in the G gain matrix. A similar procedure can be adopted to calculate k_d and g, fixing ω_f equal to the controlled mode natural frequency ω by modifying the state matrix and reducing the number of gains. In particular, setting $\omega_f = \omega$ ensures greater robustness against spillover when non-modelled modes are present. Equations (11) and (12) become respectively

$$A = \begin{bmatrix} 0 & 1 & 0 & 0 \\ -\omega^2 & -2\xi\omega & 0 & -1 \\ 0 & 0 & 0 & 1 \\ 0 & 0 & -\omega^2 & 0 \end{bmatrix}$$

$$B = \begin{bmatrix} 0 \\ 0 \\ 0 \\ 1 \end{bmatrix} C = \begin{bmatrix} 0 & 1 & 0 & 0 \\ 0 & 0 & 0 & 1 \end{bmatrix} \tag{13}$$

and

$$\mathbf{v} = G\mathbf{y} = \begin{bmatrix} k_d\, g & -2\xi_f\omega - k_d \end{bmatrix}\mathbf{y} \tag{14}$$

To obtain a unique correspondence between the gains and coefficients to be determined, ξ_f can be fixed arbitrarily and the design procedure involves only k_d and g.

3.2. Output feedback control optimal solution

The linear quadratic regulator (LQR) optimal approach applied to output feedback control problem was discussed widely in [9]. It can be applied to (10) finding the control force $\mathbf{v}$ minimizing a quadratic cost

$$J = \frac{1}{2}\int_0^\infty \left(\mathbf{z}^T Q\mathbf{z} + \mathbf{v}^T R\mathbf{v}\right) dt \tag{15}$$

where Q and R are the weighting matrices that must be positive semidefinite. Since the control action is not proportional to the whole state vector $\mathbf{z}$, in order to find the minimizing gain matrix G it is necessary to solve three matrix equations instead of a single Riccati equation. Moerder and Calise [10] proposed an iterative algorithm which solves the equations starting from an initial gain matrix G_0. Since in order to have a convergent algorithm the matrix G_0 has to stabilize the closed loop state

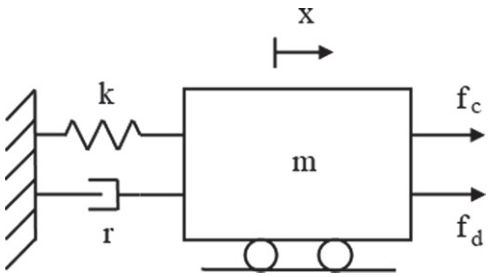

Figure 1. A single d.o.f. linear vibrating system with a disturbance (f_d) and an active control (f_c) force.

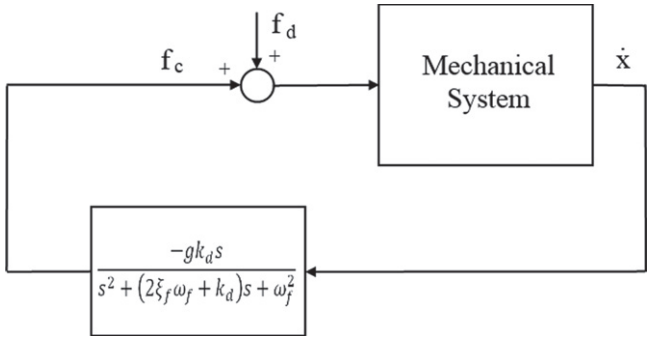

Figure 2. NDF control scheme applied to a single d.o.f. vibrating system.

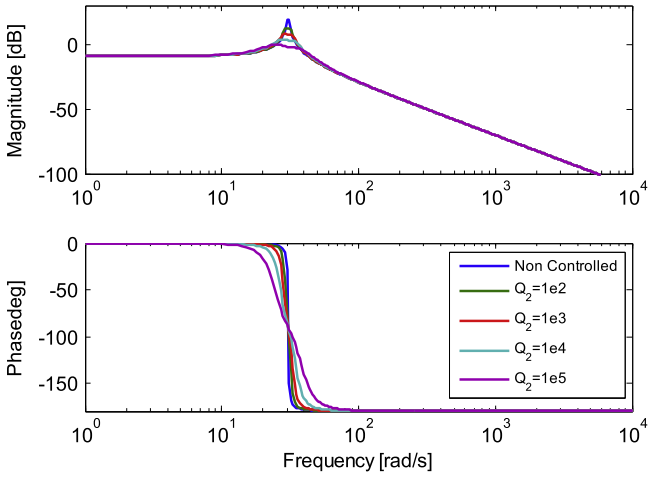

Figure 3. NDF control applied to single d.o.f. system; influence of Q_2 on the FRF between the mass displacement x and the disturbance force f_d($Q = diag\,([0,\ Q_2,\ 0,\ 0])$, $R = 1$).

space matrix

$$A^* = A - BG_0C \tag{16}$$

it could be necessary to solve the static output feedback stabilization problem using a method like the one suggested by Moore *et al* [11] and based on the Schur matrix decomposition.

3.3. Multi-d.o.f. systems

The same approach discussed in the previous paragraph can be generalized to multi-d.o.f. systems. If the number of modes

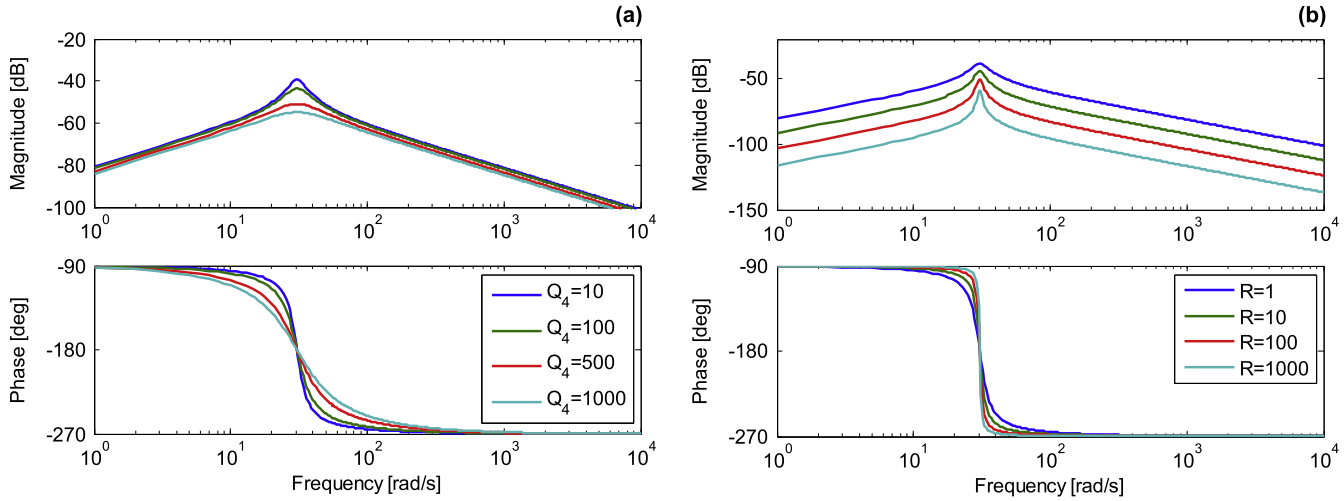

Figure 4. NDF control applied to single d.o.f. system; influence of Q_4 ($Q = diag\,([0,\ 1e3,\ 0,\ Q_4])$, $R = 1$, on the left) and influence of R ($Q = diag\,([0,\ 1e3,\ 0,\ 0])$, on the right) on the FRF between $\dot{x}$ and the control force f_c.

to be controlled is greater than one, the synthesis can in fact be made considering only the modes on which the control forces will act to increase damping. The resulting state space form is a decentralized control problem as

$$\begin{cases} \dot{\mathbf{z}} &= A\mathbf{z} + \sum_{1}^{r} B_i \mathbf{v}_i \\ \mathbf{y}_i &= \begin{bmatrix} \dot{q}_i & g_i\eta_i & g_i\dot{\eta}_i \end{bmatrix} = C_i \mathbf{z} \end{cases} \tag{17}$$

where r is the number of controlled modes and the state vector is

$$\mathbf{z} = \begin{Bmatrix} \mathbf{q} \\ \dot{\mathbf{q}} \\ g_1\eta_1 \\ g_1\dot{\eta}_1 \\ \vdots \\ g_r\eta_r \\ g_r\dot{\eta}_r \end{Bmatrix} \tag{18}$$

The state space matrix becomes

$$A = \begin{bmatrix} \mathbf{0} & \mathbf{I} & \mathbf{0} & \mathbf{0} & \mathbf{0} & \mathbf{0} & \dots \\ -K_m & -R_m & \mathbf{0} & -\begin{bmatrix} 1 \\ 0 \\ \vdots \end{bmatrix} & \mathbf{0} & -\begin{bmatrix} 0 \\ 1 \\ \vdots \end{bmatrix} & \dots \\ \mathbf{0} & \mathbf{0} & 0 & 1 & 0 & 0 & \dots \\ \mathbf{0} & \mathbf{0} & 0 & 0 & 0 & 0 & \dots \\ \mathbf{0} & \mathbf{0} & 0 & 0 & 0 & 1 & \dots \\ \mathbf{0} & \mathbf{0} & 0 & 0 & 0 & 0 & \dots \\ \vdots & \vdots & \vdots & \vdots & \vdots & \vdots & \ddots \end{bmatrix} \tag{19}$$

where K_m and R_m are respectively the modal stiffness and the modal damping matrices, while the input and observation matrices are defined respectively as

$$B_1 = \begin{bmatrix} \mathbf{0} \\ \mathbf{0} \\ 0 \\ 1 \\ 0 \\ 0 \\ \vdots \end{bmatrix} B_2 = \begin{bmatrix} \mathbf{0} \\ \mathbf{0} \\ 0 \\ 0 \\ 0 \\ 1 \\ \vdots \end{bmatrix} \tag{20}$$

and

$$C_1 = \begin{bmatrix} \mathbf{0} & [1\ 0\ \dots] & 0 & 0 & 0 & \dots \\ \mathbf{0} & \mathbf{0} & 1 & 0 & 0 & \dots \\ \mathbf{0} & \mathbf{0} & 0 & 1 & 0 & \dots \end{bmatrix}$$
$$C_2 = \begin{bmatrix} \mathbf{0} & [0\ 1\ 0\ \dots] & 0 & 0 & 0 & 0 & 0 & \dots \\ \mathbf{0} & \mathbf{0} & 0 & 0 & 1 & 0 & 0 & \dots \\ \mathbf{0} & \mathbf{0} & 0 & 0 & 0 & 1 & 0 & \dots \end{bmatrix} \tag{21}$$

For each d.o.f. the control action is computed as

$$\mathbf{v}_i = G_i \mathbf{y}_i \tag{22}$$

The algorithm can be modified in a way similar to that shown in (13) and (14) for the single d.o.f. by setting the compensator frequency equal to the controlled mode frequency. However, optimal approaches to decentralized output feedback control problems are more complicated than for centralized systems. The method proposed in [12], based on a gradient flow approach, has been tested but convergence time is strongly dependent on the covariance matrix of initial state, which must be given as input to the algorithm. Thus, it proves to be more convenient to exploit modal decoupling by applying the single d.o.f. design methodology to each controlled mode independently.

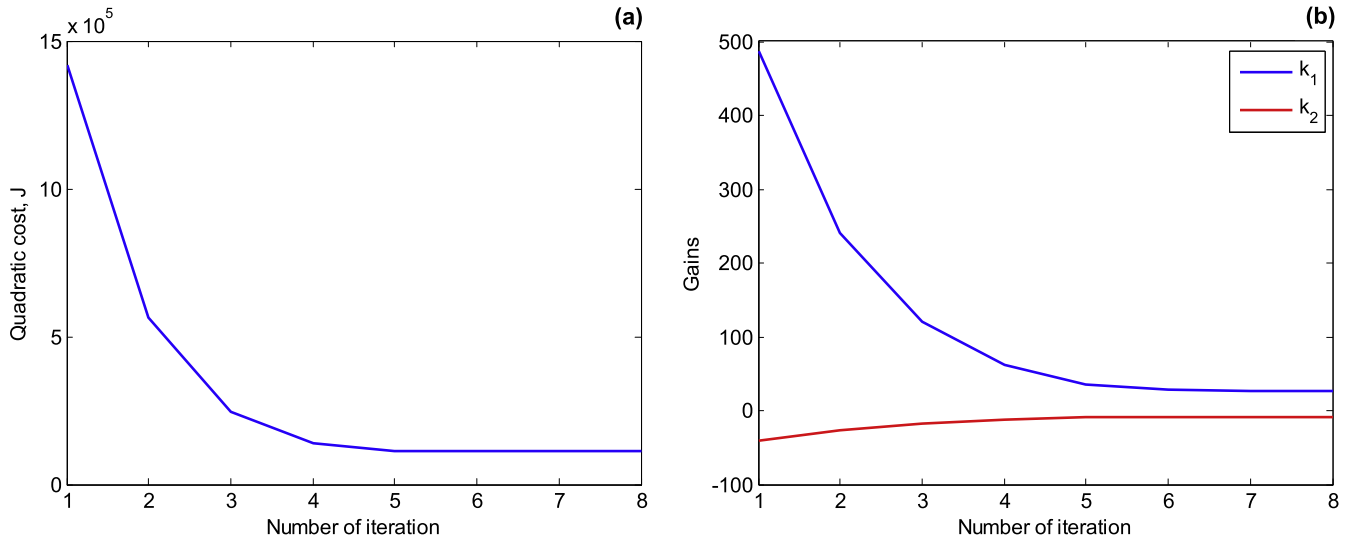

Figure 5. Output feedback control optimal solution for NDF parameters; quadratic cost J (on the left) and matrix G coefficients convergence (on the right) versus the iteration number.

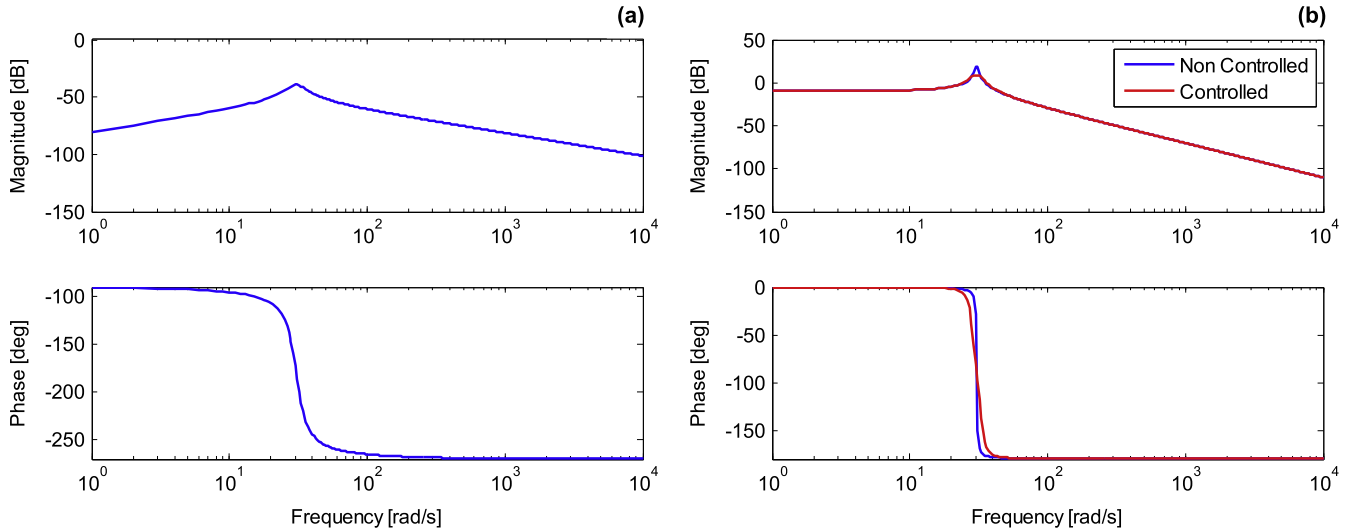

Figure 6. NDF control applied to single d.o.f. system; FRF between $\dot{x}$ and f_c (on the left) and between x and f_d (on the right).

4. Control design guidelines

The algorithm proposed in section 3 has been applied to a single d.o.f. system to show how the weighting matrices Q and R influence control performance in terms of damping increase, control effort and robustness against modelling errors. The control scheme is shown in figure 2. For this application, R is a positive scalar, while Q is set as a diagonal matrix

$$Q = diag\left(\left[Q_1,\ \ Q_2,\ \ Q_3,\ \ Q_4\right]\right) \tag{23}$$

NDF has been applied to the single d.o.f. linear system depicted in figure 1 and described by the equation of motion

$$m\ddot{x} + r\dot{x} + kx = f_c + f_d \tag{24}$$

where $m = 3.2e-2$ kg, $r = 1.8e-3$ N s m^{-1}, $k = 29.8$ N m^{-1}. Thus, the natural frequency and the damping ratio are respectively

$$\omega = \sqrt{\frac{k}{m}} = 30.5 \text{ rad s}^{-1} \tag{25}$$

$$\xi = \frac{r}{2\,m\omega} = 0.92\% \tag{26}$$

The analysis of weight influence on control performances limited the control design to the definition of parameters Q_2, Q_4 and R. Q_2 is the weight corresponding to the modal velocity which is the first variable fed back in the problem reformulation (equation (14)). As could be expected from optimal control theory, increasing the value of Q_2 results in a greater damping of the controlled system as is shown in figure 3 where the frequency response function (FRF)

Table 1. The cantilever beam model: geometrical and structural characteristics.

L (m)	J (m^4)	A (m^2)	E ($N\,m^{-2}$)	ρ ($kg\,m^{-3}$)
1.0	$7.2 \cdot 10^{-10}$	$2.4 \cdot 10^{-4}$	$7.5 \cdot 10^{10}$	2780

Table 2. The cantilever beam model: actuators, and sensors, position (distance from the clamp).

	A_1	A_2	A_3	S_1	S_2	S_3
Distance (m)	0.15	0.35	0.95	0.10	0.40	0.55

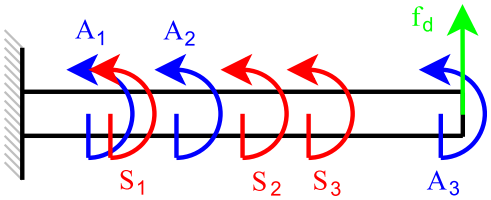

Figure 7. The cantilever beam model and the three actuators, three sensors and a disturbance force applied.

between the disturbance f_d and mass displacement x is represented for different values of Q_2.

Parameter Q_4 corresponds to the second variable fed back, $g\dot{\eta}$. Acting on Q_4, it is possible to regulate in the phase diagram the gradient of the transfer function $F_c/\dot{X}(s)$ in correspondence with the frequency ω_f, as shown in figure 4(a). This way, it is possible to extend the range of frequency in which the control action introduces a damping effect, increasing the robustness against natural frequency estimation errors. Finally, weight R allows the control effort to be balanced, as shown in figure 4(b).

5. Numerical results

5.1. Single d.o.f. system

In this section the algorithm proposed is applied first to the single d.o.f. linear system described in section 4 and then to a multi-d.o.f. system. For the second example, the methodology has been tested on a cantilever beam finite element model (FEM) in order to highlight the spillover effects and to prove the validity of the design method.

Following the procedure described in section 3, and imposing the weighting matrices $Q = diag\,[0,\ 1e3,\ 0,\ 1e1]$ and $R = 1$, and starting from the initial gain matrix $G_0 = [485.87,\ -40.00]$, the algorithm converges to the solution $G = [27.16,\ -8.02]$ in 8 iterations. The quadratic cost J decreases until variation drops below the 0.1 threshold, as shown in figure 5(a), while the gains convergence is represented in figure 5(b).

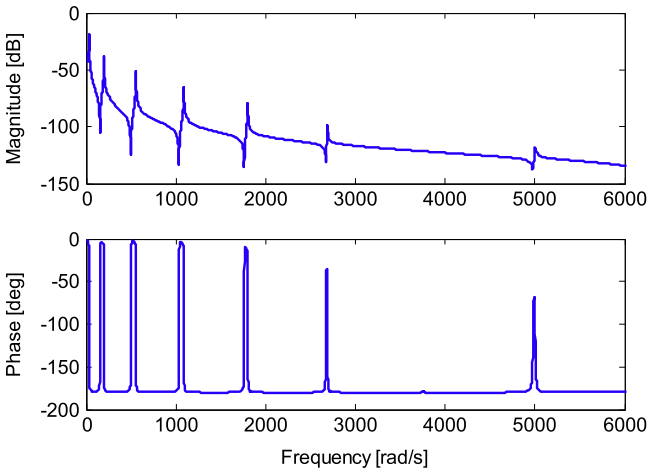

Figure 8. The cantilever beam FRF between the tip vertical displacement and the disturbance force f_d.

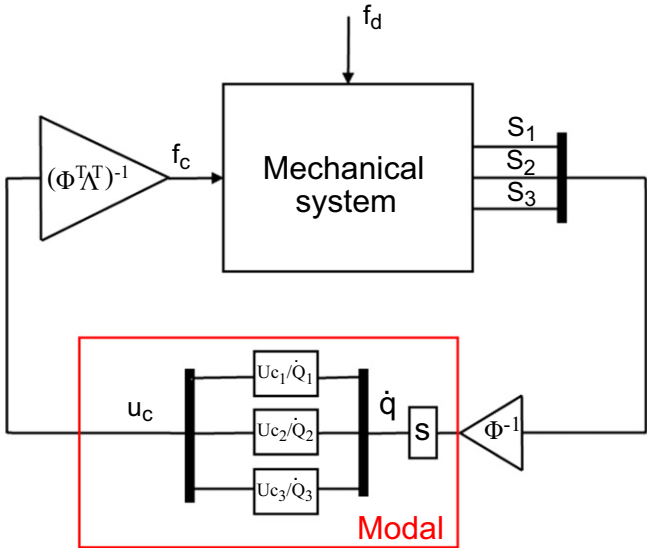

Figure 9. NDF control scheme applied to a multi-d.o.f. vibrating system.

Imposing $\xi_f = 0$ and remembering $\omega_f = \omega$, the other compensator parameters can be obtained from the matrix G through equation (14) ($g = 3.39$ and $k_d = 8.02$). In figure 6(a), for the designed compensator, the FRF between the system velocity $\dot{x}$ and the control force f_c is shown. It can be seen that the band-pass filter is centred on the system's natural frequency, and the control force rolls off for lower and higher frequencies.

In figure 6(b) the increase of damping for the controlled system is shown through the FRF between the system state x and a generic disturbance f_d. In order to obtain higher damping, it would be possible to act on the ratio between the values of matrices Q and R at the expense of the control effort.

5.2. Multi d.o.f. system

A second test has been carried out on a multi-d.o.f. system. A cantilever beam FEM has been created in order to test the

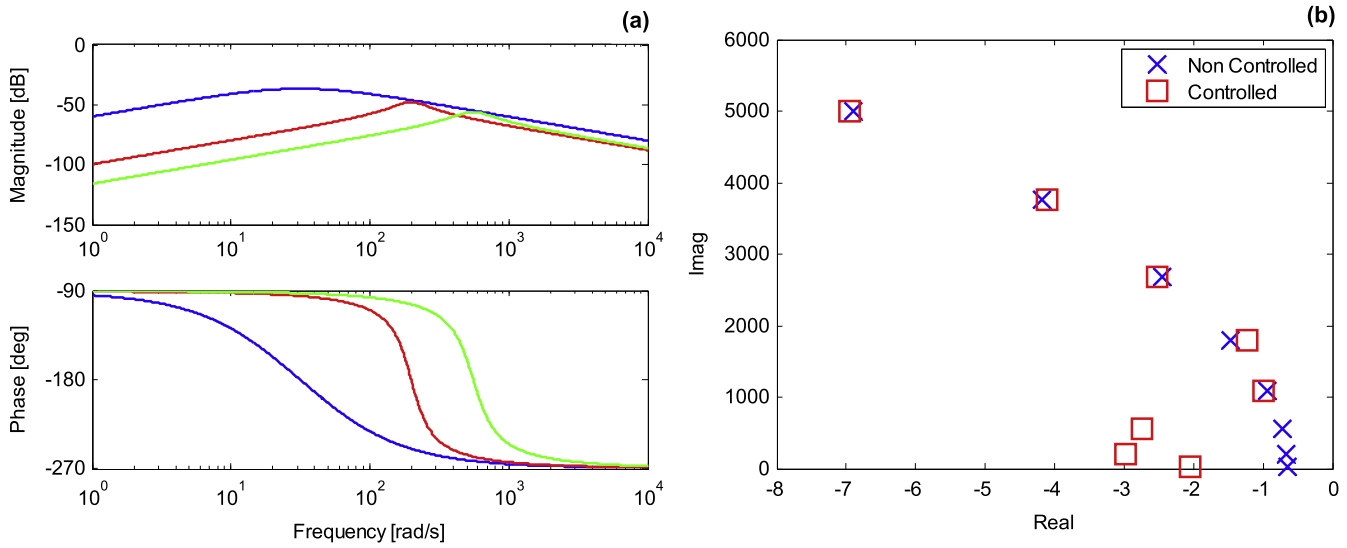

Figure 10. The cantilever beam numerical simulation (case A): transfer functions $U_{c_i}/\dot{Q}_i(s)$ of the compensators tuned on the first three modes (on the left) and poles, location for the non-controlled and controlled systems (on the right).

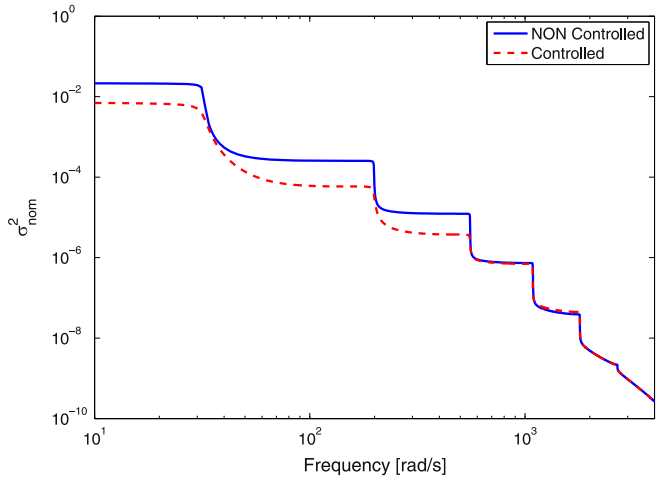

Figure 11. The cantilever beam numerical simulation (case A): cumulative mean-square response between the tip vertical displacement and the disturbance f_d for the non-controlled and controlled systems.

methodology in the presence of uncontrolled modes which can suffer from observation and control spillover. The continuous structure has been discretized with 20 nodes, equally distributed, each one with 3 d.o.f. (2 displacements and 1 rotation). The beam characteristics in terms of geometry and material are summarized in table 1. In order to obtain fully decoupled equations in modal coordinates, the damping matrix has been defined according to the Rayleigh proportional damping assumption

$$R = \alpha M + \beta K \tag{27}$$

with $\alpha = 1.3$ and $\beta = 5 \cdot 10^{-7}$. Three sensors and three actuators are placed on the structure in a generic non-collocated configuration (table 2). Both actuators (A) and sensors (S) act on the rotational d.o.f. A disturbance force (f_d) acts on the tip vertical displacement (figure 7). As an example, the FRF between the tip vertical displacement and the disturbance force acting on the same degree of freedom is shown in figure 8.

The principal coordinates are reconstructed by inverting the observation matrix describing the relationship between the modal displacements and physical measures. This way, effects related to observation spillover are taken well into account. The control scheme is represented in figure 9.

Since in this case fine tuning of the compensators on the controlled modes, natural frequencies could reduce spillover effects, k_{d_i} and g_i are chosen independently of ω_{f_i} (set equal to the generic system natural frequency ω_i). The design problem is formulated as in (13), considering only the modes to be controlled. In order to consider spillover at both high and low frequencies, two cases have been examined:

- Case A: control acting on the first three modes (modes 1, 2 and 3)
- Case B: control acting on the second three modes (modes 4, 5 and 6)The results shown below refer to the choice of weights summarized in table 3.

In figure 10(a) the transfer functions $U_{c_i}/\dot{Q}_i(j\omega)$ for the three compensators tuned on the first three modes is represented (case A).

The control action results in increased damping of the controlled modes (and a correspondent percentage peak reduction of 65%, 75% and 71%) while the effects due to spillover are negligible, thanks to the reduced contribution on higher frequency modes. Only a relatively insignificant reduction of the 5th mode damping ratio can be seen (figure 10(b)).

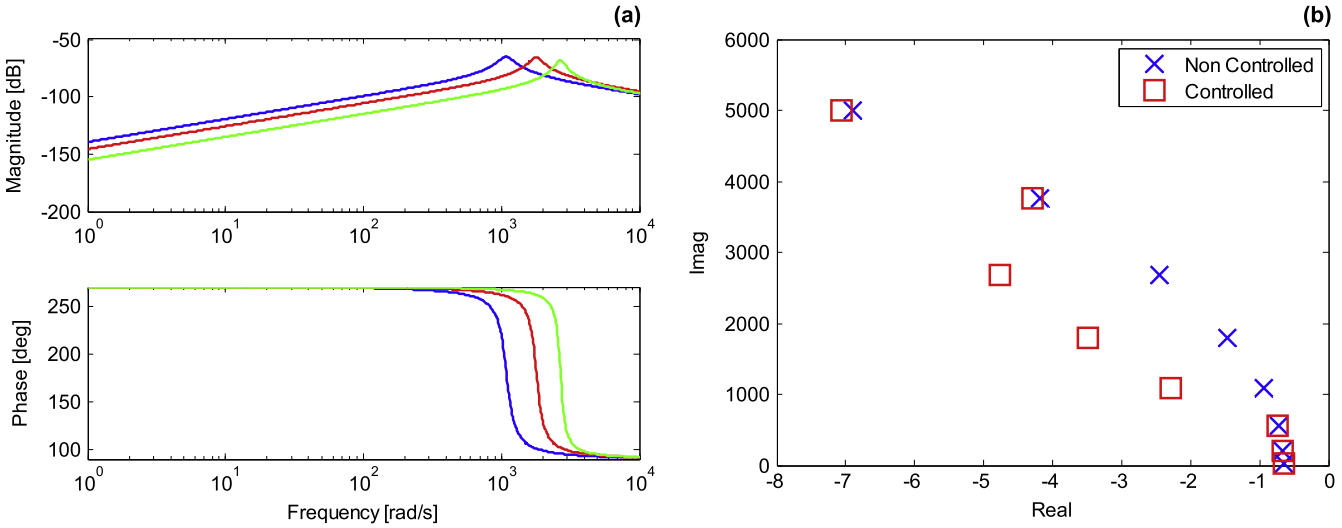

Figure 12. The cantilever beam numerical simulation (case B): transfer functions $U_{c_i}/\dot{Q}_i(s)$ of the compensators tuned on the first three modes (on the left) and poles, location for the non-controlled and controlled systems (on the right).

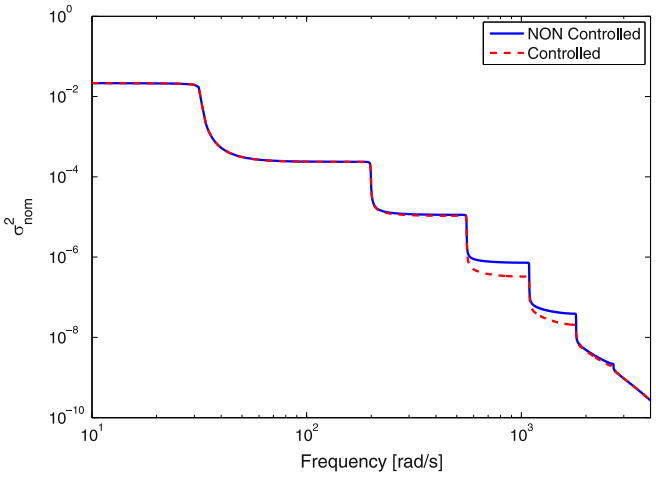

Figure 13. The cantilever beam numerical simulation (case B): cumulative mean-square response between the tip vertical displacement and the disturbance f_d for the non-controlled and controlled systems.

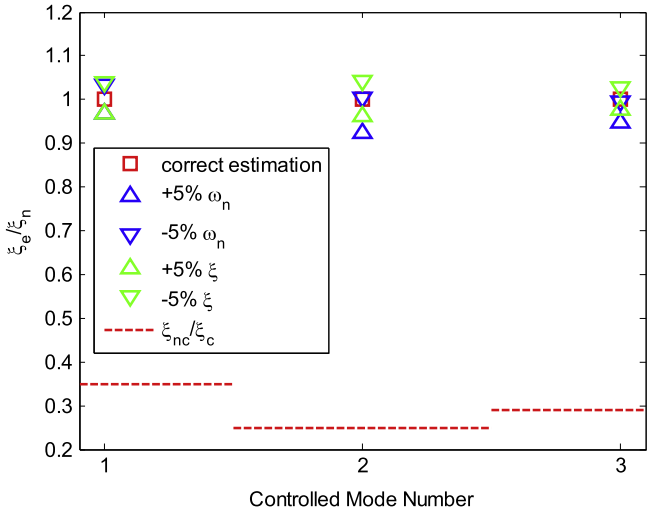

Figure 14. The cantilever beam numerical simulation (case A): robustness analysis on the first three modes, final damping ratio through an error on the natural frequencies, and damping ratios, estimation.

Control performance is evaluated comparing the cumulative mean-square response calculated as

$$\sigma^2(\omega) = \int_{\omega}^{\infty} \left(FRF(\omega)\right)^2 d\omega \qquad (28)$$

normalized with respect to the value $\sigma^2(0)$ of the non-controlled system. The results, considering the FRF between the tip vertical displacement and the external disturbance for the non-controlled and controlled systems, are shown in figure 11.

Similar considerations can be drawn with regard to case B in which the second three modes have been controlled (figure 12(a)). Control action is concentrated coherently on modes 4, 5 and 6 (percentage peak reduction of 58%, 57% and 48%), and no damping reduction appears either at lower or higher frequencies (figure 12(b)).

Also for this case, the cumulative mean-square response has been computed and shown in figure 13 for both non-controlled and controlled systems. The improvement on the 4th and 5th modes is significant compared with the effect on the 6th, which is lower owing to its limited influence on the whole FRF.

5.3. Robustness analysis

Dealing with the multi-d.o.f. simulation, and in particular case A, a robustness analysis has also been performed to evaluate the changes in performance obtained if damping ratios and natural frequencies are not estimated accurately. Referring to the beam FEM, the design of the experiment has been applied

Table 3. The cantilever beam numerical simulation: the weighting matrices for the gain matrices calculation through the optimal control approach.

Case A	Q_i	R_i	Case B	Q_i	R_i
Mode 1	$diag\left[0\ 7e1\ 0\ 5e3\right]$	1	Mode 4	$diag\left[0\ 5e1\ 0\ 5e4\right]$	1
Mode 2	$diag\left[0\ 4e1\ 0\ 1e4\right]$	1	Mode 5	$diag\left[0\ 1e2\ 0\ 1e5\right]$	1
Mode 3	$diag\left[0\ 2e2\ 0\ 5e4\right]$	1	Mode 6	$diag\left[0\ 2e2\ 0\ 1e5\right]$	1

Table 4. The cantilever beam numerical simulation: robustness analysis results.

	$+5\%\ \omega$			$-5\%\ \omega$			$+5\%\ \xi$			$-5\%\ \xi$		
Mode	**1**	**2**	**3**	**1**	**2**	**3**	**1**	**2**	**3**	**1**	**2**	**3**
ξ_{c_e}/ξ_{c_n}	0.97	0.93	0.94	1.03	1.00	1.01	0.97	0.96	0.96	1.04	1.04	1.03
ξ_{nc_i}/ξ_{c_n}	0.35	0.25	0.29	0.35	0.25	0.29	0.35	0.25	0.29	0.35	0.25	0.29
ΔF		0.938			1.069			0.940			1.071	

introducing an error of $\pm 5\%$ in the structure's modal parameters. Four cases have been tested: overestimation and underestimation of the first three natural frequencies, and overestimation and underestimation of the corresponding damping ratios. In figure 14 damping variations in the controlled modes are shown. Values have been normalized by computing the ratio between the effective (e) and the nominal (n) damping ratio obtained with a correct estimation of ω_i and ξ_i. Damping ratios always remain positive (stability is preserved) and greater than the threshold represented by the ratio between the structural damping and the nominal value (dashed red line). Moreover, cumulative power spectral densities (PSDs) of the FRF between each control force (j) and the disturbance over the $0 - 1000\ Hz$ frequency range have been evaluated

$$PSD_j = \int_0^{1000\ Hz} \left(\frac{F_{c_j}}{F_d} \right)^2 df \tag{29}$$

and the variations in the control effort have been estimated as the sum of each force's contribution normalized with respect to the nominal value

$$\Delta F = \frac{\sum_{j=1}^{3} PSD_{j,e}}{\sum_{j=1}^{3} PSD_{j,n}} \tag{30}$$

All the results are summarized in table 4. As can be seen, an increase in damping always results in increased control action and vice-versa. However, variations are in the range of $\pm 8\%$.

6. Conclusion

In this work a design methodology for an NDF compensator based on the output feedback control formulation is proposed. Thanks to an optimal approach, the design problem lies in the choice of the weighting factors of the state error and control effort matrices. The iterative algorithm, starting from a stabilizing initial gain, allows the compensator parameters to be defined. With small changes in the problem formulation, it is possible to tune the frequency of the compensator on the natural frequency of the mode to be controlled independently of the choice of the other coefficients. The method has been applied first to a single d.o.f. system; then modal decomposition allows the algorithm to be extended to a multi-d.o.f. system such as the cantilever beam FEM. Finally, a robustness analysis has been performed to show how performance changes in terms of damping and control effort when modal parameters are not correctly estimated.

References

[1] Baruh H and Meirovitch L 1983 Robustness of the independent modal-space control method. *J. Guid. Control Design* **6** 20–5

[2] Balas M J 1978 Active control of flexible systems *J. Optimiz. Theor. Appl.* **25** 415–36

[3] Caughey T K and Goh C J 1985 On the stability problem caused by finite actuator dynamics in the collocated control of large space structures *Int. J. Control* **41** 787–802

[4] Agrawal B N, Song G and Schmidt S P 1998 Experimental study of active vibration suppression if flexible structures using modular control patch *Proc. IEEE Aerospace Applications Conf. (Los Alamitos, CA)* vol 1

[5] Cazzulani G, Resta F and Ripamonti F 2011 Active modal tuned mass damper for smart structures *Eng. Lett.* **19** 297

[6] Cazzulani G, Resta F, Ripamonti F and Zanzi R 2012 Negative derivative feedback for vibration control of flexible structures *Smart Mater. Struct.* **21** 075024

[7] Soong T T and Rana S 1998 Parametric study and simplified design of tuned mass dampers *Eng. Struct.* **20** 193–204

[8] Inman D J and Friswell M I 1999 The relationship between positive position feedback and output feedback controllers *Smart. Mater. Struct.* **8** 285–91
[9] Lewis F L, Vrabie D and Syrmos V L 1995 *Optimal Control* 2nd edn (Chichester: Wiley)
[10] Calise A J and Moerder D D 1985 Convergence of a numerical algorithm for calculating optimal output feedback gains *IEEE Trans. Automatic Control* **30** 900–3
[11] Yang Y, Orsi R and Moore J B 2004 A projective algorithm for static output feedback stabilization *Proc. IFAC World Congr.* vol 1
[12] Moore J B and Jang D 1996 A gradient flow approach to decentralised output feedback optimal control *Syst. Control Lett.* **27** 223–31